

Degradation of artificial sweeteners via direct and indirect photochemical reactions

Noora Perkola¹ · Sanna Vaalgamaa^{2,5} · Joonas Jernberg^{3,6} · Anssi V. Vähätalo^{2,4}

Received: 23 October 2015 / Accepted: 16 March 2016 / Published online: 29 March 2016
© Springer-Verlag Berlin Heidelberg 2016

Abstract We studied the direct and indirect photochemical reactivity of artificial sweeteners acesulfame, saccharin, cyclamic acid and sucralose in environmentally relevant dilute aqueous solutions. Aqueous solutions of sweeteners were irradiated with simulated solar radiation (>290 nm; 96 and 168 h) or ultraviolet radiation (UVR; up to 24 h) for assessing photochemical reactions in surface waters or in water treatment, respectively. The sweeteners were dissolved in deionised water for examination of direct photochemical reactions. Direct photochemical reactions degraded all sweeteners under UVR but only acesulfame under simulated solar radiation. Acesulfame was degraded over three orders of magnitude faster than the other sweeteners. For examining indirect photochemical reactions, the sweeteners were dissolved in

surface waters with indigenous dissolved organic matter or irradiated with aqueous solutions of nitrate (1 mg N/L) and ferric iron (2.8 mg Fe/L) introduced as sensitizers. Iron enhanced the photodegradation rates but nitrate and dissolved organic matter did not. UVR transformed acesulfame into at least three products: iso-acesulfame, hydroxylated acesulfame and hydroxypropyl sulfate. Photolytic half-life was one year for acesulfame and more than several years for the other sweeteners in surface waters under solar radiation. Our study shows that the photochemical reactivity of commonly used artificial sweeteners is variable: acesulfame may be sensitive to photodegradation in surface waters, while saccharin, cyclamic acid and sucralose degrade very slowly even under the energetic UVR commonly used in water treatment.

Responsible editor: Roland Kallenborn

Electronic supplementary material The online version of this article (doi:10.1007/s11356-016-6489-4) contains supplementary material, which is available to authorized users.

✉ Noora Perkola
noora.perkola@environment.fi

¹ Finnish Environment Institute (SYKE), Laboratory Centre, Hakuninmaantie 6, FI-00430 Helsinki, Finland

² Department of Environmental Sciences, University of Helsinki, P.O. Box 65 (Viikinkaari 1), FI-00014 Helsinki, Finland

³ Department of Environmental Sciences, University of Helsinki, Niemenkatu 73, FI-15140 Lahti, Finland

⁴ Department of Biological and Environmental Science, University of Jyväskylä, P.O. Box 35 (Survontie 9), FI-40014 Jyväskylä, Finland

⁵ Present address: Sito Oy, Tuulikuja 2, FI-02100 Espoo, Finland

⁶ Present address: Ordior Oy, Konalantie 47 A, FI-00390 Helsinki, Finland

Keywords Artificial sweeteners · Acesulfame · Sucralose · Photochemical reactions · Photolytic half-life · Solar simulation

Abbreviations

ACS	acesulfame
CDOM	chromophoric dissolved organic material
CYC	cyclamic acid
ES	electrospray ionization (ES ⁻ and ES ⁺ : negative and positive ES)
Fe(II)	ferrous iron
Fe(III)	ferric iron
LC-MS	liquid chromatography–mass spectrometry
FWHM	full width at half-maximum
LC-MS/MS	liquid chromatography–tandem mass spectrometry
R	mass resolution
SAC	saccharin

SCL	sucralose
SI	Supporting Information
SIM	single ion monitoring
$t_{1/2}$	(photolytic) half-life
TOF MS	time-of-flight mass spectrometer
TQ MS	triple quadrupole mass spectrometer
t_R	retention time
UV	ultraviolet
UVR	ultraviolet radiation

Introduction

Acesulfame (ACS), saccharin (SAC), cyclamic acid (CYC) and sucralose (SCL) are used as artificial sweeteners. These sweeteners enter to environment through wastewater and have been detected in aquatic environment and drinking water (Berset and Ochsenbein 2012; Buerge et al. 2009; Mawhinney et al. 2011; Perkola and Sainio 2014; Müller et al. 2011; Scheurer et al. 2009; van Stempvoort et al. 2011). This has caused concerns about their persistence and effects in the environment (Eriksson Wiklund et al. 2012; Hjorth et al. 2010; Hugget and Stoddard 2011; Soh et al. 2011).

Photochemical reactions can potentially be an important pathway for degradation of artificial sweeteners in water treatment and in the surface waters. In water treatment, ultraviolet radiation (UVR; <290 nm) can degrade ACS directly (Coiffard et al. 1999; Nödler et al. 2013; Scheurer et al. 2014), whereas degradation of SCL requires photocatalytic conditions (Keen et al. 2013; Sang et al. 2014).

Those artificial sweeteners absorbing photolytic radiation themselves can potentially undergo direct photochemical reactions in water treatment (Coiffard et al. 1999; Nödler et al. 2013; Scheurer et al. 2014, Zepp and Cline 1977). In surface waters, the direct photochemistry of sweeteners is likely low, because the sweeteners are colourless and may also absorb solar ultraviolet radiation (>290 nm) poorly (Coiffard et al. 1999).

Even if the sweeteners do not absorb solar radiation, they may undergo indirect photochemical transformations with transients (e.g. hydroxyl radicals) produced by sensitizers. A primary sensitizer of surface waters is chromophoric part of dissolved organic matter (DOM; Hoigne et al. 1988; Paul et al. 2004). Surface water contains also nitrate, which produces hydroxyl radicals with an apparent quantum yield of 0.017 (Machado and Boule 1995). Ferric iron, Fe(III), is a versatile sensitizer. It can form complexes e.g. with DOM or organic pollutants and increase absorption of solar radiation (Maloney et al. 2005; Shapiro 1966; Xiao et al. 2015). UVR reduces complexed Fe(III) to ferrous iron, Fe(II), and can oxidize the organic ligand down to CO₂ through ligand-to-metal charge transfer reactions (Sun and Pignatello 1993). The oxidation of

Fe(II) by O₂ or H₂O₂ (the latter is the Fenton reaction) regenerates Fe(III) for another catalytic cycle and generates hydroxyl radicals, which can potentially react with artificial sweeteners (Zepp et al. 1992).

The aim of our study was to examine photochemical transformation of ACS, SCL, SAC and CYC in environmentally relevant low concentrations under conditions found in the surface waters and in water treatment by UVR.

Material and methods

Standards and reagents

The analytical native and mass-labelled (acesulfame-*d*₄ potassium, ¹³C₆-saccharin, cyclamic acid-*d*₁₁ and sucralose-*d*₆) standards of acesulfame potassium salt, saccharin, cyclamic acid and sucralose were purchased from Toronto Research Chemicals Inc. (North York, Ontario, Canada). Liquid chromatography–mass spectrometry (LC-MS) grade methanol and ammonium acetate used in the LC eluents were manufactured by Fluka Analytical (Buchs, Switzerland). The iron(III) sulfate (Fe₂(SO₄)₃·5H₂O; 97 %) and potassium nitrate (KNO₃; 99 %, p.a.) used in the photolysis test solutions were manufactured by Aldrich (Steinheim, Germany) and Merck (Darmstadt, Germany), respectively.

Sample collection

The surface waters used in the simulated solar irradiation study were collected into 1-L polypropylene bottles from Lake Päijänne (62.14°N 25.77°E; June 2011) and River Tuusula (60.33°N 24.92°E, August 2011). Lake Päijänne is a large lake in central Finland, with low organic content (chemical oxygen demand 7.8 mg/L). River Tuusula is a small, eutrophic river in southern Finland. The pH, conductivity, turbidity and the concentration of nitrate were 7.0, 6.7 mS/m, 1.3 FNU and 77 µg of N/L, respectively, in the lake sample. In river water sample, the corresponding values were 7.4, 20 mS/m, 10 FNU and 220 µg of N/L, respectively. The water samples were stored frozen, and thawed and filtered with GF/A 1.6-µm glass fibre filters (Whatman, Kent, UK) before the irradiation experiments.

Absorption spectra

For absorption measurements, CYC, SCL, ACS and SAC were dissolved in deionised water at concentrations 1.0, 1.5, 1.6 and 2.0 g/L, respectively. The absorption spectra were scanned with a Shimadzu UV-2550 UV–vis spectrophotometer from 200 to 800 nm at 1-nm intervals with 2-nm slit width in 1- or 10-cm quartz cuvettes against deionised water blank.

The natural logarithms of absorption coefficients (m^{-1}) were calculated as:

$$\text{Absorption coefficient} = (2.303A)l^{-1} \quad (1)$$

where 2.303 converts the 10-based logarithm of absorption to natural logarithm, A is the absorbance, and l is the length of the light path, 0.01 or 0.1 m.

The molar absorptivity (ϵ ; L/mol cm) of each compound was derived from the absorbance spectrum:

$$\epsilon = A(cl)^{-1} \quad (2)$$

where c is the molar concentration (mol/L) and l is a path length of 1 cm.

Irradiation experiments

For irradiation experiments, the solutions of artificial sweeteners were enclosed in 13-mL quartz or glass tubes without headspace closed with ground glass stoppers. Quartz tubes (irradiation samples) were irradiated at horizontal position in a deionised water bath at 20 °C. Glass tubes were covered with aluminium foil and stored in a refrigerator (4 °C; unexposed samples) or in the water bath (dark control samples).

Environmental photochemistry was assessed by irradiating the sweeteners for 96 or 168 h with simulated solar radiation generated by an Atlas Suntest CPS+ solar simulator equipped with a xenon arc lamp and a UV-filter cutting off the wavelengths below 290 nm. Solar simulator emitted 302 W/m² at the spectral band from 290 to 500 nm, which is 11-times more than the mean annual irradiance at sea level over the entire planet Earth (27.3 W/m² at the same spectral band; Chu and Liu 2009; Vaalgamaa et al. 2011). Therefore, the 96- and 168-h irradiations corresponded to 44.2 and 77.4 days of average solar radiation on the surface of Earth. For assessing direct photochemical reactions, ACS, SAC, CYC and SCL were dissolved in deionised water as a mixture, where the concentration of each sweetener was 87, 110, 84 and 460 µg/L, respectively. The same mixture dissolved in Fe(III) solution (2.8 mg/L of Fe) or in surface water (lake and river water) was used to assess the indirect photochemistry mediated by Fe and indigenous sensitizers including DOM, respectively (Wang et al. 2008).

UVR irradiation was performed with the same instrument after the removal of the UV-filter and the replacement of the xenon arc with a 15-W low-pressure mercury lamp (UV-technik Speziallampen GmbH, Wolfsberg, Germany), which emitted mainly at 254 nm like many lamps used in water treatment (UVC Low-Pressure Lamp Fact Sheet). The samples were irradiated typically for 24 h, but a shorter period from 1 to 240 min was also used for ACS. In order to study the potential phototransformation products of sweeteners, each sweetener was dissolved separately to the concentrations

of 220 µg/L (ACS), 87 µg/L (SAC), 86 µg/L (CYC) and 440 µg/L (SCL). The sweeteners were dissolved in deionised water for assessing direct photoreactions. Indirect photoreactions were examined in Fe(III) solution (2.8 mg/L of Fe) or in nitrate (1 mg/L of N, i.e. 4.4 mg/L of NO₃⁻) solution. All experiments included reaction solutions without sweeteners as blank samples.

Estimation of half-lives

Reaction rate constants (k) were calculated as

$$k = \ln\left(\frac{C_0}{C_t}\right)t^{-1} \quad (3)$$

where t is the irradiation time in seconds, C_0 is the initial and C_t the final concentration of the compound after irradiation. In the simulated solar irradiation tests, the rate constants were calculated as an average of the irradiations (96 and 168 h), except 96 h alone was used for Fe(III) experiment.

Photolytic $t_{1/2}$ representative for global surface waters at the depth of 0 m was calculated as

$$t_{1/2} = \ln 2 \times t(\ln C_0 - \ln C_t)^{-1} \quad (4a)$$

where t represents 44.2 or 77.4 days of average sunshine received during 96- and 168-h irradiation with the solar simulator.

If the concentration of sweetener in the irradiated sample was not statistically different from that in the corresponding dark control, the photodegradation of the sweetener was undetectable, i.e. below the precision of our analytical method defined as standard deviation (SD) of replicated samples. If any photodegradation took place, the potential minimum concentration of sweetener in the irradiated sample at time t (C_t) was C_0 -SD. In this case, the potential minimum photolytic $t_{1/2}$ was:

$$t_{1/2} = \ln 2 \times t(\ln C_0 - \ln(C_0 - \text{SD}))^{-1} \quad (4b)$$

The SDs for the measurement of the replicated samples prepared for irradiation experiments ($n = 11$ – 12) were 4.2 µg/L or 5 % (CYC), 18 µg/L or 4 % (SCL), 6.3 µg/L or 6 % (SAC) and 4.4 µg/L or 5 % (ACS).

Analytics

Prior to instrumental analysis, each sample was filtered with nylon filters (ø25 mm, pore size 0.2 µm; Corning, NY, USA). The filtrates received surrogate standards to final concentrations of 300 ng/mL for acesulfame- d_4 potassium, 400 ng/mL for ¹³C₆-saccharin, 300 ng/mL for cyclamic acid- d_{11} and 2000 ng/mL for sucralose- d_6 .

Samples were analysed with liquid chromatography–tandem mass spectrometry (LC-MS/MS). Separation was performed with an Acquity Ultra Performance LC (Waters, Milford, MA, USA) in an Acquity BEH C18 analytical column (1.7 μm , 2.1 \times 50 mm). The analytes were eluted with a gradient consisting of 2 mM ammonium acetate in water and in methanol during a 3.0-min run. The gradient started with 0.1 % of eluent methanol, followed by an increase to 99.9 % methanol over 2 min. The column was flushed with 99.9 % methanol for 0.3 min, after which the initial conditions were applied in 0.1 min, and the column was stabilized for 0.6 min. Eluent flow rate was 0.4 mL/min. The column temperature was set to 40 °C and the sample temperature to 7 °C. Injection volume was 7.5 μL . The samples were quantified with a Xevo Triple Quadrupole (TQ) MS (Waters) using negative electrospray ionization (ES⁻). Multiple reaction monitoring mode (resolution (R)=0.75 Da) was applied with specific mass transitions for each sweetener (Table S1 in Supporting Information; SI). The MS method is described in detail elsewhere (Perkola and Sainio 2014).

The chemical composition of phototransformation products was studied with an orthogonal time-of-flight mass spectrometer (TOF MS) Micromass LCT Premier XE (Micromass MS Technologies, Manchester, UK). The potential elemental compositions of the tentative phototransformation products were calculated by MassLynx software (Waters) (Nurmi et al. 2012). The analysis was performed in a W optics mode with both negative and positive ES. The LC conditions were the same as with Xevo TQ MS. The mass resolution of the instrument was >11,000 full width at half-maximum height (FWHM), and the measured mass range (m/z) was 50–600 in a centroid mode. The mass accuracy was at least ± 5 mDa (Nurmi et al. 2012). Capillary voltages were 3000 and 2600–3000 V for ES⁺ and ES⁻, respectively. Desolvation gas (N_2) flow was 800 L/h and temperature 350 °C. The temperature of ionization source was 120 °C. After the tentative phototransformation products were identified with TOF MS, the changes in their concentrations during irradiations were analysed based on peak area with TQ MS in a single ion monitoring (SIM) mode (R =1.0 Da FWHM), and their fragmentation was studied with a product ion scan (R =2.9–15.0 Da FWHM). To be able to compare the areas of the transformation products from different LC-MS runs, they were normalised to original parent compound peak area in a sample that was not irradiated.

Results and discussion

Absorbance at 200–800 nm

ACS and SAC absorbed primarily in the UVC-region of the spectrum but also above 290 nm (Fig. S1 and Table S2, SI).

This indicates that they could potentially undergo direct photochemical reactions when exposed to UVR or even to sunlight. CYC and SCL did not absorb in the solar UV region. Therefore, direct photochemical reactions were not expected for CYC and SCL under solar radiation. We used molar absorptivities (Eq. 2, Fig. S1, Table S2) to calculate the absorption coefficients of sweeteners at 254 nm at the concentrations used later in the UVR irradiation experiments. The absorption coefficients at 254 nm for ACS (220 ng/L), SAC (87 ng/L), CYC (86 ng/L) and SCL (440 ng/L) were 0.76 m^{-1} , 0.14 m^{-1} , $2.6 \times 10^{-5} \text{ m}^{-1}$ and $6.2 \times 10^{-4} \text{ m}^{-1}$, respectively (Table S2, SI). Based on these values, the potential for direct photolysis at 254 nm was highest for ACS and SAC and lowest for CYC and SCL.

Photolysis with simulated solar radiation

Simulated solar radiation reduced the concentration of ACS in deionised water with the rate constant of $2.2 \times 10^{-7} \text{ s}^{-1}$ (Fig. 1 and Table 1) indicating photochemical transformation through direct reactions. Simulated solar radiation did not mediate the photolysis of SAC, SCL and CYC in deionised water (Table 1). These results indicate that solar radiation can photodegrade ACS but not SAC, SCL and CYC through direct photoreactions.

When the sweeteners were irradiated in lake and river water, their photodegradation rates were similar to that in deionised water (Fig. 1 and Table 1). The similarity of rate constants indicates that the indigenous sensitizers such as DOM of nitrate in our surface water samples did not promote indirect photoreactions, and direct photolysis was the primary removal mechanism for ACS. This is supported by a study of Soh et al. (2011) where the addition of natural organic matter did not affect the phototransformation of ACS.

Fe(III) stimulated indirect phototransformation of ACS, SAC and CYC under solar radiation (Table 1) indicating indirect photochemistry mediated by Fe. For example, the reaction rate of ACS was more than twice higher in Fe(III) solution than in deionised water (Table 1). These results indicate that solar radiation can photodegrade sweeteners (even poorly reactive SAC and CYC) through Fe-mediated indirect reactions in surface waters high in Fe.

The degradation rates of ACS and SAC in Fe(III) solution decreased substantially after 96-h irradiation (Fig. 1 and Fig. S2, SI). This may be explained by the photochemical depletion of dissolved O_2 during prolonged irradiation with Fe (Miles and Brezonik 1981; Xie et al. 2004). In the absence of O_2 , photochemically reduced Fe remains as Fe(II), and the photochemical catalysis based on O_2 and the redox cycle of Fe stops (Miles and Brezonik 1981; Zepp et al. 1992;

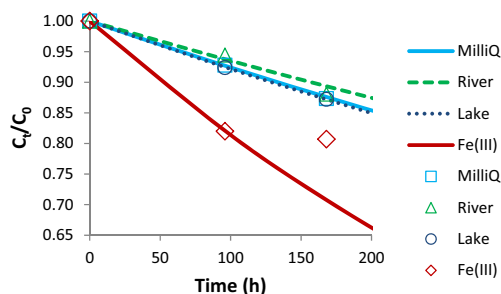


Fig. 1 Decrease of acesulfame in lake, river, deionised water and ferric iron solution under simulated solar radiation. The *lines* represent calculated concentrations at time *t* (hours) versus the concentration before irradiation (C_t/C_0), and the *markers* represent the measured values. The measured value of Fe(III) solution at 168 h ignored for the first order fitting (see text for details)

Sun and Pignatello 1993). The depletion of O_2 was possible in our quartz tubes closed without headspace, but is not relevant in natural surface waters, which receive a constant supply of O_2 from the atmosphere.

Iron redox chemistry may explain also the results of CYC, which showed an apparent reduction in the early part of irradiation and recovery in the prolonged (168 h) irradiation (Table S3, SI). The apparent reduction of CYC may be explained by photochemistry-induced precipitation of Fe(III) oxides with concomitant complexation of CYC on them in the early part of irradiation (von Wachenfeldt et al. 2008; Helms et al. 2013). In the latter part of irradiation, the recovery of CYC may be related to the reduction of Fe(III) to Fe(II) and

Table 1 Reaction rate constants (k , s^{-1}) under simulated solar radiation and photolytic half-lives in water surface layer ($t_{1/2}$, day) for acesulfame (ACS), saccharin (SAC), cyclamic acid (CYC) and sucralose (SCL) in deionised water, ferric iron solution (Fe(III)) and filtered surface water (river and lake)

		ACS	SAC	CYC	SCL
Deionised water	k (s^{-1})	2.2×10^{-7}	ND	ND	ND
	$t_{1/2}$ (day)	380	>860	>1000	>1300
Fe(III)	k (s^{-1})	5.7×10^{-7}	1.4×10^{-6}	2.4×10^{-7}	ND
	$t_{1/2}$ (day)	250	110	370	>1300
River	k (s^{-1})	1.9×10^{-7}	ND	ND	ND
	$t_{1/2}$ (day)	420	>860	>1000	>1300
Lake	k (s^{-1})	2.3×10^{-7}	ND	ND	ND
	$t_{1/2}$ (day)	380	>860	>1000	>1300

$t_{1/2}$ represent the calculated half-life in the average radiation values in Earth's surface waters

The rate constants and $t_{1/2}$ were calculated from 96- and 168-h irradiations using Eq. 3, except Fe(III) which were calculated from the 96-h irradiation

The photolytic $t_{1/2}$ were calculated either using Eq. 4a or 4b. The relative SDs of SAC, CYC and SCL were 6, 5 and 4 %, respectively

ND not determined. Photodegradation below the analytical precision

simultaneous release of CYC (Helms et al. 2013). It is hard to assess of environmental relevance of these reactions, but the co-precipitation of CYC with Fe(III) oxides can transport it from water column to sediments, where reduction of Fe(III) to Fe(II) may release it back to solution.

The photodegradation rates of sweeteners found under solar simulator can be translated into rates found in the surface waters under natural solar radiation by accounting for the relative differences in the photolytic irradiance between the two sources of radiation (Eq. 4). Simulated solar radiation decreased the concentration of ACS by 12–19 % in 168 h (Table S3, SI) which represents 77.4 days of average, latitude and season independent sunshine on Earth. At the surface waters at the depth of 0 m, the photolytic $t_{1/2}$ of ACS can be calculated (Eq. 4a) to be 360 days (12 months) in lake water or 390 days (13 months) in river water (Table 1). In a recent study, significantly shorter near-surface summer $t_{1/2}$ were suggested for ACS, approximately 180 days in deionised water at pH 7 and 17 days in filtered river water (pH 8) (Gan et al. 2014). In that study, sterilization and filtration decreased the degradation rate of ACS, and the near surface summer $t_{1/2}$ was even shorter, only 9 days, in unfiltered river water. Also, nitrate enhanced the solar phototransformation of ACS (Gan et al. 2014). In our experiments, the nitrate concentrations in river and lake water (220 and 77 $\mu\text{g/L}$, respectively) did not provide a sufficient amount of hydroxyl radicals to enhance the photolysis of ACS. In fact, the $t_{1/2}$ were longer in natural waters compared to deionised water. The different $t_{1/2}$ of ACS in surface water in our study and the study of Gan et al. (2014) could be partly explained by the high nitrate concentration in the Chinese river (9.5 mg/L in filtered and 16 mg/L in unfiltered water, representing 2100 and 3600 $\mu\text{g N/L}$, respectively), and probably by the low microbial activity in our frozen and filtered surface waters. In addition, $t_{1/2}$ of our study represents the average planetary phototransformation rates that are independent on latitude, whereas the outdoor study of Gan et al. (2014) was performed on latitude 39.13°N.

The photolysis of SAC, SCL and CYC was absent or within the analytical precision (coefficients of variations of 6, 4 and 5 %, respectively) in deionised and surface waters. Their minimum $t_{1/2}$ calculated based on the SDs ($n=11$ or 12; Eq. 4b) ranged from 2.4 years (>860 days) of SAC to 3.6 years (>1300 days) of SCL (Table 1). If the surface waters would have the same stimulatory effect as our Fe(III) solution, the photolytic $t_{1/2}$ of SAC and CYC are 110 and 370 days (Table 1). In some surface waters, such as nearly 20 % of water samples collected from Finnish rivers (Xiao et al. 2015), the concentration of total Fe exceeds that of Fe(III) solutions used in our irradiation experiments. Even in the

presence of high Fe, the photolytic $t_{1/2}$ of SAC, SCL and CYC are long.

In perspective of the low photoreactivity of artificial sweeteners in surface waters, they can indeed be used as tracers of municipal wastewater in the environment (Buerge et al. 2009; Mawhinney et al. 2011; Müller et al. 2011; van Stempvoort et al. 2011; Wolf et al. 2012). For ACS, the calculated photolytic $t_{1/2}$ refers to the very surface (depth of 0 m) in water column. In reality, the $t_{1/2}$ are much longer, because the highly water-soluble sweeteners are expected to distribute evenly in the surface mixing layer and are exposed only periodically to the highest irradiances at the very surface. In addition, the intensity of solar radiation and thus the $t_{1/2}$ varies by latitude, altitude and season.

Photolysis under UVR

The UVR irradiations with a low-pressure mercury lamp reduced the concentrations of all the four sweeteners dissolved in deionised water (Figs. 2 and S3, SI). Photodegradation of ACS took place within minutes at a rate constant (k) of $9.9 \times 10^{-3} \text{ s}^{-1}$ (Fig. 2, the first ‘deionised water’ row of Table 2). The degradation of ACS followed first order kinetics (Fig. 2) which is typical for direct photolysis (Zepp and Cline 1977). Assuming that the photochemical degradation on SAC, CYC and SCL also followed first order kinetics, their calculated rate constants were three to four orders of magnitude lower than for ACS (the first ‘deionised water’ row of Table 2). These results indicate that all the artificial sweeteners were degraded by direct photoreactions with UVR, but the rates were low except for ACS.

Similarly to our study, ACS has been reported to degrade under low-pressure mercury lamp irradiations (Scheurer et al. 2014; Sang et al. 2014; Soh et al. 2011). Our rate constant for ACS (Table 1) is similar to the $6.3 \times 10^{-3} \text{ s}^{-1}$ determined in a recent study (Scheurer et al. 2014), but twice as high as the $2.38 \times 10^{-3} \text{ s}^{-1}$ that has

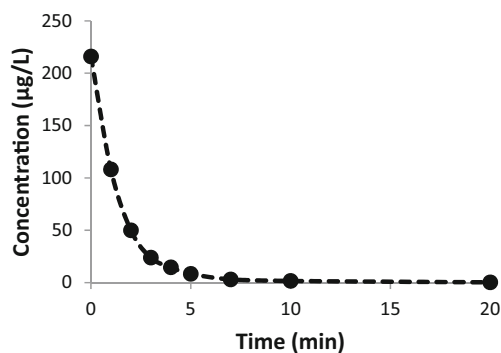


Fig. 2 Degradation of acesulfame under UV irradiation

Table 2 The reaction rate constants (k ; unit s^{-1}) of acesulfame (ACS), saccharin (SAC), cyclamic acid (CYC) and sucralose (SCL) in deionised water, ferric iron (Fe(III)) and nitrate (NO_3^-) solutions in the samples irradiated with UVC

	ACS	SAC	CYC	SCL
Deionised water	9.9×10^{-3}	9.2×10^{-6}	3.6×10^{-6}	4.7×10^{-7}
Fe(III)	-	$\geq 6.8 \times 10^{-5}$	1.0×10^{-5}	8.4×10^{-7}
NO_3^-	-	7.1×10^{-6}	3.2×10^{-6}	ND

“-” indicates that rate was not calculated

ND not determined. Photodegradation below the analytical precision

been reported earlier (Soh et al. 2011). However, the latter was based on a five-hour irradiation within borosilicate bottles, which transmit only little UVR <350 nm (Schott Borofloat 33 - Optical Properties) where ACS absorbs (Fig. S1, SI). Our $t_{1/2}$ for ACS (1.2 min) is shorter than 15 min obtained earlier by Coiffard et al. (1999). The difference in $t_{1/2}$ may be related to the spectrum and intensity of the light source used but not reported by Coiffard et al. (1999). Like in this study, SCL has been reported rather persistent to direct photolysis at 254 nm (and 350 nm) earlier (Soh et al. 2011; Torres et al. 2011). Our study extends the earlier observations of SCL to CYC and SAC, which both photodegrade poorly via direct photochemical reactions under UVR.

Nitrate solution did not stimulate additional indirect photochemical transformation of any sweetener examined (Table 1 and Table S4, SI). In our experiments, the absorption coefficient of nitrate (1 mg/L of N) at 254 nm was at the same level (0.34 m^{-1} , Vaalgamaa et al. 2011) as those of ACS and SAC solutions (0.76 and 0.14 m^{-1} ; Table S2, SI), and higher than those of CYC and SCL (2.6×10^{-5} , and $6.2 \times 10^{-4} \text{ m}^{-1}$; Table S2, SI). Our results indicate that under conditions used in our study, UVC irradiance nitrate does not produce sufficient amount of hydroxyl radicals to effectively react with sweeteners.

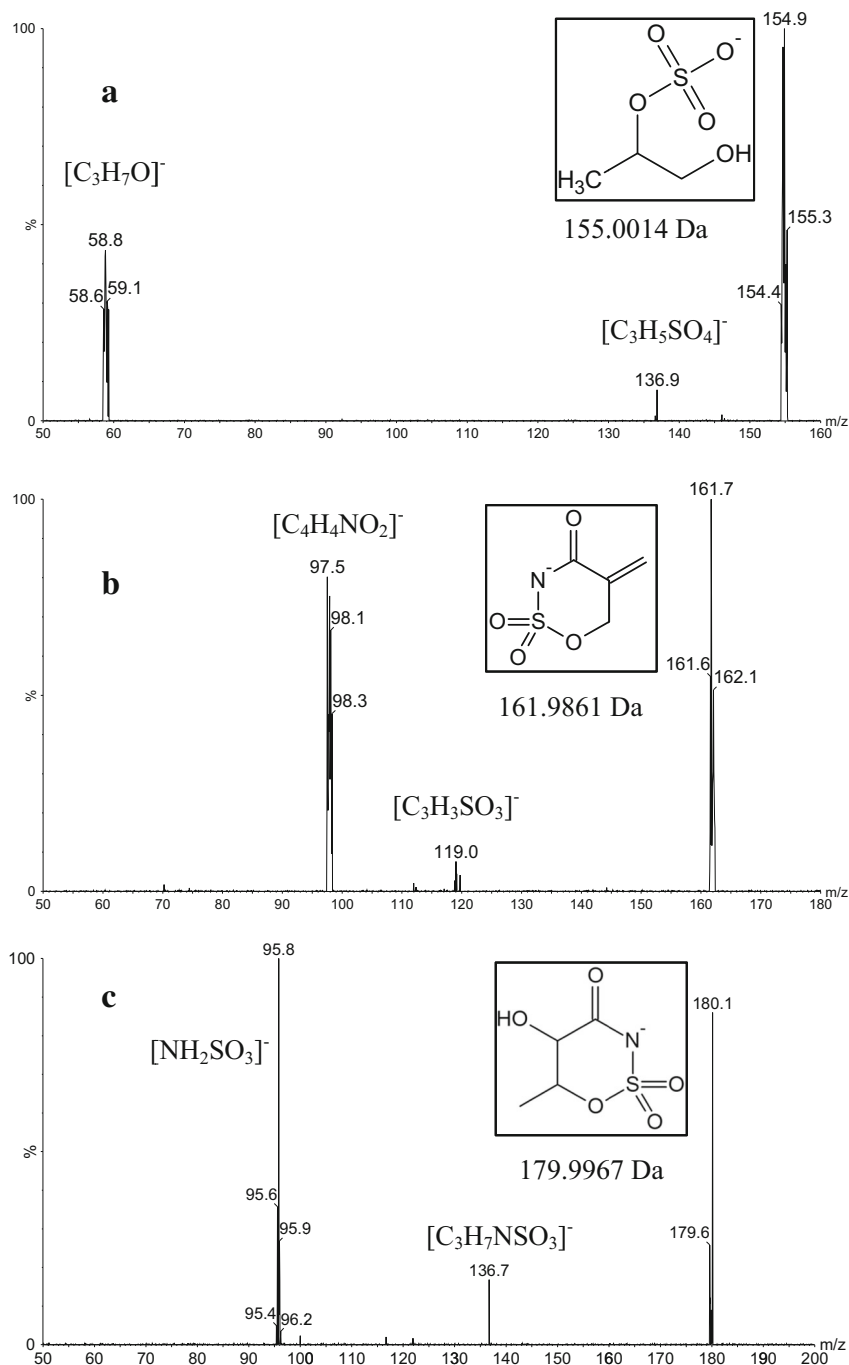
In the irradiated Fe(III) solutions, the degradation and the rate constants of SAC, CYC and SCL roughly doubled compared to those in the respective deionised water solutions indicating that Fe(III) acted as a sensitizer for phototransformations (Table 2 and Table S4, SI). Irradiation of Fe(III) solution with dissolved O_2 leads to hydroxyl radicals generated by the Fenton reaction (Zepp et al. 1992). Highly reactive hydroxyl radicals react relatively non-selectively and can explain the increased rates of degradation for the all sweeteners (Table 2). The increase in rate constant was the fastest for SAC (Table 2), which may form a complex with Fe(III) (Yilmaz et al. 2001) and react additionally via the ligand-to-metal charge transfer mechanism (Sun and

Pignatello 1993). Furthermore, a recent study showed efficient phototransformation of SCL in the presence of TiO_2 , another producer of hydroxyl radicals (Sang et al. 2014). The earlier and our study indicate that efficient producers of hydroxyl radicals (Fe(III) , TiO_2) can enhance photodegradation of those sweeteners, which react poorly through direct photoreactions.

In conclusion, the direct photochemical degradation of ACS can be rapid under UVR, and germicidal UV water treatment is a promising treatment to remove ACS

from drinking water and wastewater. Although SAC and CYC were degraded under UVC irradiation in our study, their photochemical transformation rate is low, and direct photolysis of SAC and CYC would be ineffective during conventional UV water treatment. The direct photolysis of SCL is too slow to significantly occur during the UV treatment process. The photo degradation of SAC, CYC and SCL under UVC and therefore during germicidal UV water treatment could be improved with Fe(III) . However, although the reactivity

Fig. 3 Fragmentation and potential molecular structures of acesulfame phototransformation product ions m/z 155 (a), m/z 162 (b) and m/z 180 (c) with TQ MS. The monoisotopic mass of the phototransformation product ion $[\text{M-H}]^-$ is presented below the molecule. The proposed elemental compositions of fragment ions are presented in brackets



of the sweeteners with hydroxyl radicals is relatively high, the organic material inhibits the oxidation reactions (Toth et al. 2012). Therefore, the hydroxyl radical enhanced photodegradation in water treatment might be efficient only after removal of the organic material.

Phototransformation products

In the deionised water solutions of ACS irradiated with UVR, ES– TOF MS detected three transformation products (m/z 155.001, 161.987 and 179.998; Fig. S4–S8, SI). The largest ions were only detected in irradiated samples, but the ion m/z 155.001 was also detected in dark control samples. The peak area of m/z 155.001 was over three times higher (area=55) in the 120-min irradiated sample than in the 168-h dark control sample (area=16), and was not detected in the unexposed sample that had been stored in refrigerator (Fig. S7). In other words, the ion appeared at 20 °C without irradiation and is therefore not solely a photochemical product of ACS, but UVR enhanced its formation. Phototransformation products at m/z 50–600 were not found for SAC, CYC or SCL in the UVC-irradiated samples after 24 h (data not shown). This could be caused by the fact that some compounds did not decompose enough resulting in only small amounts of transformation products. It is also possible that our analytical methods failed to detect transformation products. The ability of the C18 analytical column to retain polar compounds is limited, and very polar transformation products could not be concentrated in the column. Also, the ionization of the transformation products may be low in ESI. In addition, some product ions might have been under m/z 50 and thus outside our mass range.

The measured masses of ACS transformation products (m/z 155.001, 161.987 and 179.998) are close to the monoisotopic masses of $C_3H_7SO_5$ (155.0014 Da), $C_4H_4SNO_4$ (161.9861 Da) and $C_4H_6SNO_5$ (179.9967 Da), respectively. In TQ MS, the ion m/z 155.001 fragmented into m/z 59 and 137 (Fig. 3a). The ion m/z 161.987 broke into two fragments (m/z 98 and 119; Fig. 3b), while m/z 179.998 fragmented into two major ions (m/z 96 and 137; Fig. 3c). The predicted tentative molecular structures of m/z 155.001, 161.987 and 179.998 are hydroxypropanol sulfate, iso-ACS and hydroxylated ACS, respectively (Fig. 3). When high concentrations of ACS have been irradiated, two of the MS fragmentation ions, m/z 96 (or amidosulfonic acid) of hydroxylated ACS and m/z 137 of hydroxypropanyl sulfate have been found (Sang et al. 2014; Scheurer et al. 2014).

The kinetics of the photodegradation of ACS dissolved in deionised water and the formation of transformation products was examined in a separate irradiation experiment with UVR, where irradiation produced hydroxylated ACS (m/z 179.998) within the first minutes (Fig. 4). On the basis of the relative peak areas compared to the area of ACS in the unexposed sample ($A_{ACS, i}$), the concentration of hydroxylated ACS

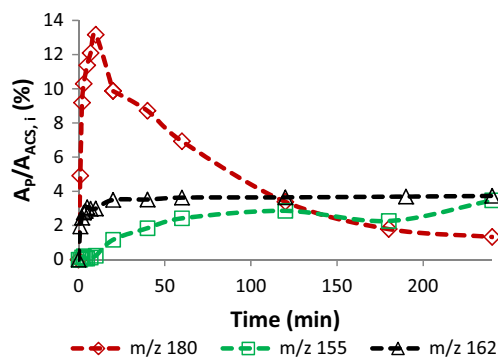


Fig. 4 Formation and elimination of acesulfame phototransformation products under UV irradiation presented as the peak area of the product ion (AP) versus the peak area of acesulfame before irradiation ($A_{ACS, i}$) in percent. m/z 155, 162 and 180 are hydroxypropanyl sulfate, iso-acesulfame and hydroxylated acesulfame, respectively

began to decrease after ten minutes when measured as an m/z 180 ion with the TQ MS (Fig. 4), and was not detected after 24 h (Fig. S9, SI). Irradiation generated iso-ACS (m/z 162) at relatively slow rate and resulted in a rather stable concentration from 60 to 240 min (Fig. 4). Also, hydroxypropanyl sulfate (m/z 155) concentration increased slowly during the irradiation (Fig. 4) and was still detectable after 24-h UVC irradiation (Fig. S9, SI). Hydroxypropanyl sulfate and hydroxylated ACS were also detected in the samples irradiated with solar simulator for 168 h, although both ions were disturbed by the matrix compounds in the surface water samples (Fig. S10–S11, SI). The proposed molecular structures, hydroxypropanyl sulfate and iso-ACS, have no chromophores making them resistant to UVR, whereas the ketone group of the hydroxylated ACS can absorb photons and result in phototransformation.

All the three transformation products found in our study were detected in recently published studies as well. Sang et al. (2014) reported ten product ions including m/z 180 and 154 under photo catalytic reaction, whereas Scheurer et al. (2014) detected five product ions including m/z 161.9867 and 179.9972 with conventional UVC irradiation, and Gan et al. (2014) ten major intermediates including m/z 180. We applied lower, more environmentally relevant ACS concentrations compared to other groups and conclude that the most prevalent transformation products are iso-acesulfame, hydroxylated acesulfame and hydroxypropanyl sulfate.

Acknowledgments This study was financed by the association of Maa-ja vesiteknikan tuki ry (Grant 23511). Dr. Anna-Lea Rantalainen, Dr. Jukka Pellinen and Santeri Savolainen are commended for the access to and help with the LC-TOF MS instrument. Janne Kontinen is thanked for the assistance in the laboratory.

This study was funded by the association Maa-ja vesiteknikan tuki ry.

Authors' contributions The manuscript was written through contributions of all the authors. All the authors have given approval to the final version of the manuscript.

References

- Berset J, Ochsenbein N (2012) Stability considerations of aspartame in the direct analysis of artificial sweeteners in water samples using high-performance liquid chromatography–tandem mass spectrometry (HPLC–MS/MS). *Chemosphere* 88:563–569. doi:10.1016/j.chemosphere.2012.03.030
- Buerge IJ, Buser H-R, Kahle M, Müller MD, Poiger T (2009) Ubiquitous occurrence of the artificial sweetener acesulfame in the aquatic environment: an ideal chemical marker of domestic wastewater in groundwater. *Environ Sci Technol* 43:4381–4385. doi:10.1021/es900126x
- Chu SX, Liu LH (2009) Analysis of terrestrial solar radiation energy. *Sol Energy* 83:1390–1409. doi:10.1016/j.solener.2009.03.011
- Coiffard CAC, Coiffard LJM, De Roeck-Holtzhauer YMR (1999) Photodegradation kinetics of acesulfame-K solutions under UV light: effect of pH. *Z Lebensm Unters Forsch A* 208:6–9. doi:10.1007/s002170050367
- Eriksson Wiklund A-K, Breitholtz M, Bengtsson B-E, Adolfsen-Erici M (2012) Sucralose—an ecotoxicological challenger? *Chemosphere* 86:50–55. doi:10.1016/j.chemosphere.2011.08.049
- Gan Z, Sun H, Wang R, Hu H, Zhang P, Ren X (2014) Transformation of acesulfame in water under natural sunlight: joint effect of photolysis and biodegradation. *Water Res* 64:113–122. doi:10.1016/j.watres.2014.07.002
- Helms JR, Mao J, Schmidt-Rohr K, Abdulla H, Mopper K (2013) Photochemical flocculation of terrestrial dissolved organic matter and iron. *Geochim Cosmochim Acta* 121:398–413. doi:10.1016/j.gca.2013.07.025
- Hjorth M, Hansen JH, Camus L (2010) Short-term effects of sucralose on *Calanus finmarchicus* and *Calanus glacialis* in Disko Bay, Greenland. *Chem Ecol* 26:385–393. doi:10.1080/02757540.2010.504672
- Hoigne J, Faust BC, Haag WR, Zepp RG (1988) Aquatic humic substances as sources and sinks of photochemically produced transient reactants. In: MacCarthy P (ed) Suflet IH. American Chemical Society, Aquatic Humic Substances, pp 363–381
- Hugget DB, Stoddard KI (2011) Effects of the artificial sweetener sucralose on *Daphnia magna* and *Americamysis bahia* survival, growth and reproduction. *Food Chem Toxicol* 49:2575–2579. doi:10.1016/j.fct.2011.06.073
- Keen OS, Linden KG (2013) Re-engineering an artificial sweetener: transforming sucralose residuals in water via advanced oxidation. *Environ Sci Technol* 47:6799–6805. doi:10.1021/es304339u
- Machado F, Boule P (1995) Photonitration and photonitrosation of phenolic derivatives included in aqueous solution by excitation of nitrite and nitrate ions. *J Photochem Photobiol A* 86:73–80. doi:10.1016/1010-6030(94)03946-R
- Maloney KO, Morris DP, Moses CO, Osburn CL (2005) The role of iron and dissolved organic carbon in the absorption of ultraviolet radiation in humic lake water. *Biogeochemistry* 75:393–407. doi:10.1007/s10533-005-1675-3
- Mawhinney DB, Young RB, Vanderford BJ, Borch T, Snyder SA (2011) Artificial sweetener sucralose in U.S. drinking water systems. *Environ Sci Technol* 45:8716–8722. doi:10.1021/es202404c
- Miles CJ, Brezonik PL (1981) Oxygen consumption in humic-colored waters by a photochemical ferrous-ferric catalytic cycle. *Environ Sci Technol* 15:1089–1095. doi:10.1021/es00091a010
- Müller CE, Gerecke AC, Alder AC, Scheringer M, Hungerbühler K (2011) Identification of perfluoroalkyl acid sources in Swiss surface waters with the help of the artificial sweetener acesulfame. *Environ Pollut* 159:1419–1426. doi:10.1016/j.envpol.2010.12.035
- Nödler K, Hillebrand O, Krzysztof I, Strahtmann M, Schiperski F, Zirlwagen J, Licha T (2013) Occurrence and fate of the angiotensin II receptor antagonist transformation product valsartan acid in the water cycle—a comprehensive study with selected β -blockers and the persistent anthropogenic wastewater indicators carbamazepine and acesulfame. *Water Res* 47:6650–6659. doi:10.1016/j.watres.2013.08.034
- Nurmi J, Pellinen J, Rantalainen A-L (2012) Critical evaluation of screening techniques for emerging environmental contaminants based on accurate mass measurements with time-of-flight mass spectrometry. *J Mass Spectrom* 47:303–312. doi:10.1002/jms.2964
- Paul A, Hackbarth S, Vogt RD, Röder B, Burnison BK, Steinberg CEW (2004) Photogeneration of singlet oxygen by humic substances: comparison of humic substances of aquatic and terrestrial origin. *Photochem Photobiol Sci* 3:273–280. doi:10.1039/B312146A
- Perkola N, Sainio P (2014) Quantification of four artificial sweeteners in Finnish surface waters with isotope-dilution mass spectrometry. *Environ Pollut* 184:391–396. doi:10.1016/j.envpol.2013.09.017
- Sang Z, Jiang Y, Tsoi Y-K, Leung KS-Y (2014) Evaluating the environmental impact of artificial sweeteners: a study of their distributions, photodegradation and toxicities. *Water Res* 52:260–274. doi:10.1016/j.watres.2013.11.002
- Scheurer M, Brauch H, Lange FT (2009) Analysis and occurrence of seven artificial sweeteners in German waste water and surface water and in soil aquifer treatment (SAT). *Anal Bioanal Chem* 394:1585–1594. doi:10.1007/s00216-009-2881-y
- Scheurer M, Schmutz B, Happel O, Brauch H-J, Wülser R, Storck FR (2014) Transformation of the artificial sweetener acesulfame by UV light. *Sci Total Environ* 481:425–432. doi:10.1016/j.scitotenv.2014.02.047
- SCHOTT Borofloat 33 - Optical Properties. SCHOTT Technical Glass Solutions GmbH, Germany. http://www.schott.com/borofloat/english/download/borofloat33_opt_en_web.pdf. Accessed 23 March 2016.
- Shapiro J (1966) The relation of humic color to iron in natural waters. *Verh Int Verein Limnol* 16:477–484
- Soh L, Connors KA, Brooks BW, Zimmerman J (2011) Fate of sucralose through environmental and water treatment processes and impact on plant indicator species. *Environ Sci Technol* 45:1363–1369. doi:10.1021/es102719d
- Sun Y, Pignatello JJ (1993) Photochemical reactions involved in the total mineralization of 2,4-D by $\text{Fe}^{3+}/\text{H}_2\text{O}_2/\text{UV}$. *Environ Sci Technol* 27:302–310. doi:10.1021/es00039a010
- Torres CI, Ramakrishna S, Chao C-A, Nelson KG, Westerhoff P, Krajmalnik-Brown R (2011) Fate of sucralose during wastewater treatment. *Environ Eng Sci* 28:325–331. doi:10.1089/ees.2010.0227
- Toth JE, Rickman KA, Venter AR, Kiddle JJ, Mezyk SP (2012) Reaction kinetics and efficiencies for the hydroxyl and sulfate radical based oxidation of artificial sweeteners in water. *J Phys Chem A* 116:9819–9824. doi:10.1021/jp3047246
- UVC Low-Pressure Lamps Fact Sheet. Updated 01/2013. UV-Technik Speziallampen GmbH, Germany. http://www.uvtechnik.com/uploads/media/UVC_low_pressure_lamps_inkjet.pdf Accessed 14 May 2014.
- Vaalgamaa S, Vähätalo AV, Perkola N, Huhtala S (2011) Photochemical reactivity of perfluorooctanoic acid (PFOA) in conditions representing surface water. *Sci Total Environ* 409:3043–3048. doi:10.1016/j.scitotenv.2011.04.036
- van Stempvoort DR, Roy JW, Brown SJ, Bickerton G (2011) Artificial sweeteners as potential tracers in groundwater in urban environments. *J Hydrol* 401:126–133. doi:10.1016/j.jhydrol.2011.02.013
- von Wachenfeldt E, Sobek S, Bastviken D, Tranvik LJ (2008) Linking allochthonous dissolved organic matter and boreal lake sediment carbon sequestration: the role of light-mediated flocculation. *Limnol Oceanogr* 53:2416–2426. doi:10.4319/lo.2008.53.6.2416
- Wang Y, Zhang P, Pan G, Chen H (2008) Ferric ion mediated photochemical decomposition of perfluorooctanoic acid (PFOA) by 254 nm

- UV light. *J Hazard Mater* 160:181–186. doi:[10.1016/j.jhazmat.2008.02.105](https://doi.org/10.1016/j.jhazmat.2008.02.105)
- Wolf L, Zwiener C, Zemann M (2012) Tracking artificial sweeteners and pharmaceuticals introduced into urban groundwater by leaking sewer networks. *Sci Total Environ* 430:8–19. doi:[10.1016/j.scitotenv.2012.04.059](https://doi.org/10.1016/j.scitotenv.2012.04.059)
- Xiao Y-H, Rake A, Hartikainen H, Vahatalo AV (2015) Iron as a source of color in river waters. *Sci Total Environ* 536:914–923. doi:[10.1016/j.scitotenv.2015.06.092](https://doi.org/10.1016/j.scitotenv.2015.06.092)
- Xie H, Zafirou OC, Cai W-J, Zepp RG, Wang Y (2004) Photooxidation and its effects on the carboxyl content of dissolved organic matter in two coastal rivers in the southeastern United States. *Environ Sci Technol* 38:4113–4119. doi:[10.1021/es035407t](https://doi.org/10.1021/es035407t)
- Yilmaz VT, Topcu Y, Yilmaz F, Thoene C (2001) Saccharin complexes of Co(II), Ni(II), Cu(II), Zn(II), Cd(II) and Hg(II) with ethanolamine and diethanolamine: synthesis, spectroscopic and thermal characteristics. Crystal structures of $[\text{Zn}(\text{ea})_2(\text{sac})_2]$ and $[\text{Cu}_2(\mu\text{-dea})_2(\text{sac})_2]$. *Polyhedron* 20:3209–3217. doi:[10.1016/S0277-5387\(01\)00930-5](https://doi.org/10.1016/S0277-5387(01)00930-5)
- Zepp RG, Cline DM (1977) Rates of direct photolysis in aquatic environment. *Environ Sci Technol* 11:359–366. doi:[10.1021/es60127a013](https://doi.org/10.1021/es60127a013)
- Zepp RG, Faust BC, Hoigne J (1992) Hydroxyl radical formation in aqueous reactions (pH 3–8) of iron(II) with hydrogen peroxide: the photo-Fenton reaction. *Environ Sci Technol* 26:313–319. doi:[10.1021/es00026a011](https://doi.org/10.1021/es00026a011)